nature photonics

Article

https://doi.org/10.1038/s41566-025-01779-x

Perturbation-resilient integer arithmetic using optical skyrmions

Received: 2 August 2024

Accepted: 18 September 2025

Published online: 27 October 2025

Check for updates

An Aloysius Wang [1] ✉, Yifei Ma [1], Yunqi Zhang[1], Zimo Zhao [1], Yuxi Cai[1], Xuke Qiu[1], Bowei Dong [2] & Chao He [1] ✉

The decline of Moore's law coupled with the rise of artificial intelligence has recently motivated research into photonic computing as a high-bandwidth, low-power strategy to accelerate digital electronics. However, many modern-day photonic computing strategies are analogue, making them susceptible to noise and intrinsically difficult to scale. Optical skyrmions offer a route to overcome these limitations through digitization in the form of a discrete topological number that can be assigned to the analogue optical field. Apart from an intrinsic robustness against perturbations, optical skyrmions represent a new medium that has yet to be fully exploited for photonic computing, namely, spatially varying polarization. Here we propose and experimentally demonstrate a method for performing perturbation-resilient integer arithmetic with optical skyrmions and passive optical components, achieving discrete mathematical operations directly using optical skyrmions without external energy input.

Recent developments in structured light have enabled the generation of optical skyrmions[1–18], which include complex spatially varying polarization fields that carry information through a topological number taking an integer value. Optical skyrmions have three crucial properties that make them ideal candidates for high-density data transfer[13], namely, the ability to interface with digital information given the discrete nature of the skyrmion number, a robustness to perturbations and the potential to store arbitrarily large integers within a single localized analogue optical field.

These same reasons also make optical skyrmions (here referring specifically to Stokes skyrmions) a natural candidate for computation, with its integer-valued topological number offering a route to digital photonic computing in a way that transcends the usual bitwise framework of digital electronics. Moreover, compared with existing photonic computing strategies, which predominantly modulate the amplitude, phase and wavelength, complex spatially varying polarization fields represent an untapped dimension that can be independently manipulated and, therefore, has the potential to increase bandwidth substantially. This is especially relevant given the growing recognition of untapped spatial degrees of freedom as a means to advance photonic technologies, with free-space optical skyrmions being one such approach[19,20].

The central reason for exploring the use of optical skyrmions in photonic computing is, however, their resistance to noise and perturbations, which arises from the integer-valued nature of the skyrmion number. The topological robustness of skyrmions has already been established in various domains, including magnetic skyrmions[21–23], and more recently, non-local quantum skyrmions[24,25], where the idea of using skyrmions to digitize information is developed from a different perspective. In the setting of optical skyrmions carried through polarization fields, the study of topological robustness has also recently garnered attention[26], with a degree of protection already verified for propagation through a number of different media[8,12,27]. This robustness is particularly relevant to photonic computing, which has, so far, remained analogue and, therefore, susceptible to noise. Take, for instance, the following three common photonic accelerators. The accumulation of random phase errors in Mach–Zehnder interferometer meshes[28,29], thermal crosstalk in microring resonator weight banks[30,31] and low optical contrast in phase-change-material-based photonic crossbar arrays[32] lead to degraded signal-to-noise ratio in large-size

[1]Department of Engineering Science, University of Oxford, Oxford, UK. [2]Institute of Microelectronics (IME), Agency for Science, Technology and Research (A*STAR), Singapore, Republic of Singapore. ✉e-mail: aloysius.wang@gmail.com; chao.he@eng.ox.ac.uk

https://doi.org/10.1038/s41566-025-01779-x

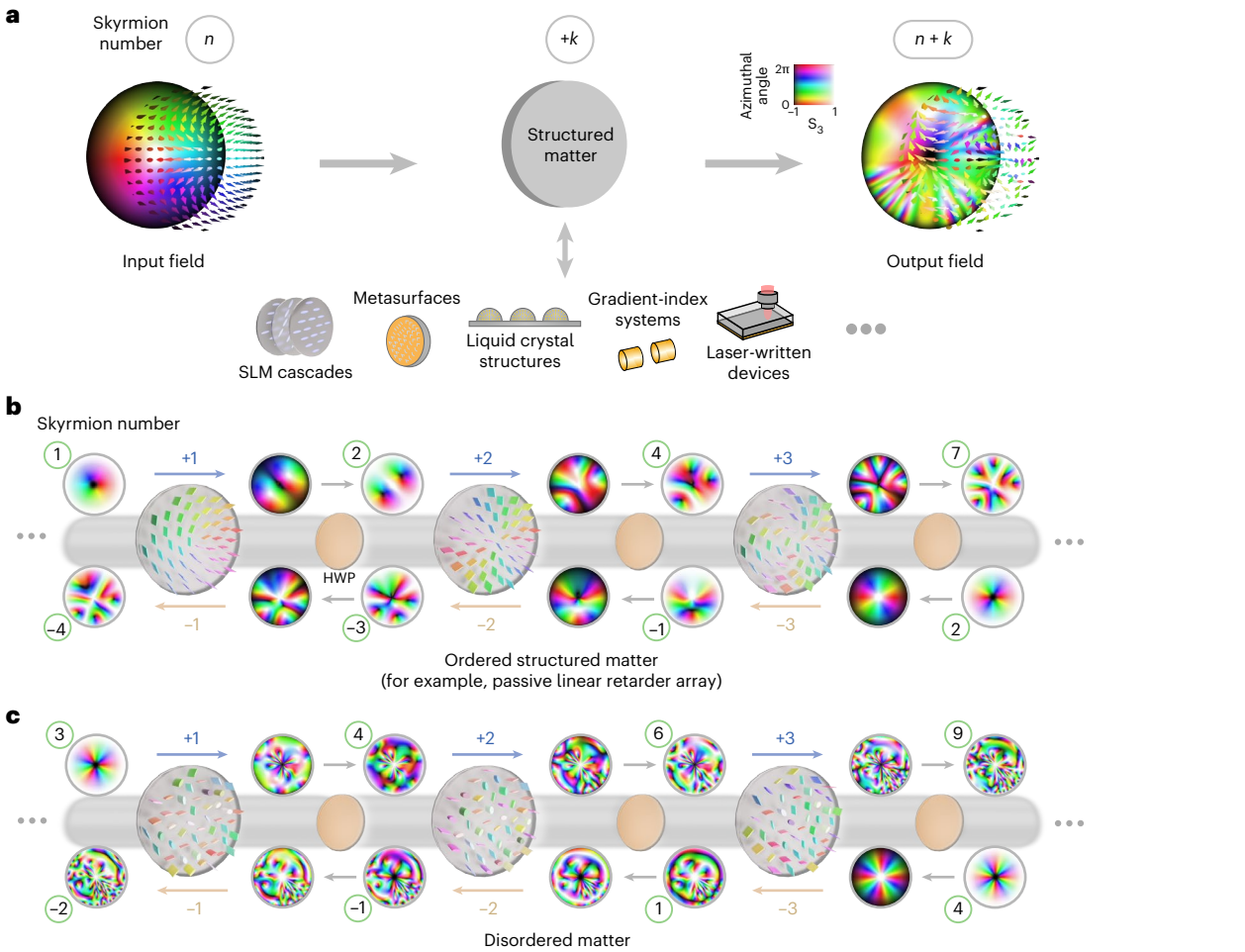

Fig. 1 | Concept. a, An optical skyrmion of arbitrary order n passing through specially designed passive structured matter can have the effect of addition or subtraction by an arbitrary integer, $n \mapsto n \pm k$ (only $n \mapsto n + k$ is shown here). Note that the same medium can be used to perform both addition and subtraction. Such structured matter can be realized in many different ways including SLM cascades, metasurfaces, inkjet printing of liquid crystal structures, gradient-index systems, direct laser writing of birefringent structures in silica and more. This figure also depicts the Stokes fields of a standard Néel-type skyrmion passing through such a medium. Throughout this paper, colour is used to represent the azimuthal angle on the Poincaré sphere (PS), and saturation to represent height (similar to ref. 13). **b**, Stokes fields of skyrmions passing through different adders of the first, second and third orders, and their respective skyrmion numbers. The linear retarder array described in the main text is used as an example, with spatially varying material properties illustrated using cylinders, where the local-axis orientation determines the shape and colour, and local retardance determines the height. Half-wave plates (HWPs) that control addition and subtraction are also shown (see the main text for details). **c**, Adders of the first, second and third orders using highly disordered materials, demonstrating the robustness of our proposed adder to imperfections of the medium. Here we consider perturbations to the linear retarder arrays that respect the conditions proposed in the main text, resulting in ellipticity of the axes and changes in retardance. Note that the chosen disorder here is merely an example that abstractly represents an arbitrary level of distortion.

implementations, circumventing the scalability of these architectures. Even with progress in device innovation[33,34], system calibration and control algorithm optimization to minimize errors[35,36], almost all photonic accelerators demonstrated so far have remained small in size (typically less than four inputs by four outputs). Although recent breakthroughs have enabled larger-scale architectures[37,38], it has been noted that noise remains a key challenge and a limiting factor for high-throughput data manipulation in photonic chips due to the use of analogue photonic signals in computing. Last, although the spatial degrees of freedom have been utilized for computation-related applications through orbital angular momentum before[39–41], these approaches do not exhibit the same robustness to noise as they are generally linear-algebraic rather than topological in nature. Computing using optical skyrmions is, therefore, a promising solution that offers greater scalability through improved stability against noise.

Motivated by this possibility, we describe here a class of structured matter (see the 'Structured matter design using a general transformation law of skyrmions' section) that, when restricted to particular types of input skyrmion, behaves as adders/subtractors (Fig. 1a) and provide experimental evidence supporting this fact. Note that the same medium can perform both addition and subtraction, but we adopt the term 'adder' throughout this paper for brevity. We would also like to emphasize that skyrmions are not topologically protected through the types of structured matter described in this paper, which have been specially designed to manipulate the skyrmion number. However, the topological nature of the skyrmion gives rise to resilience against perturbations in a different form, namely, the material parameters have flexibility to fluctuate without affecting the medium's ability to perform arithmetic (see the 'Structured matter design using a general transformation law of skyrmions' section). As mentioned above, this resilience of function is of key importance in photonic computing. Such structured matter can be realized using continuously varying retarders with specific structures on their boundary and offer a reliable way of manipulating the skyrmion number without external

https://doi.org/10.1038/s41566-025-01779-x

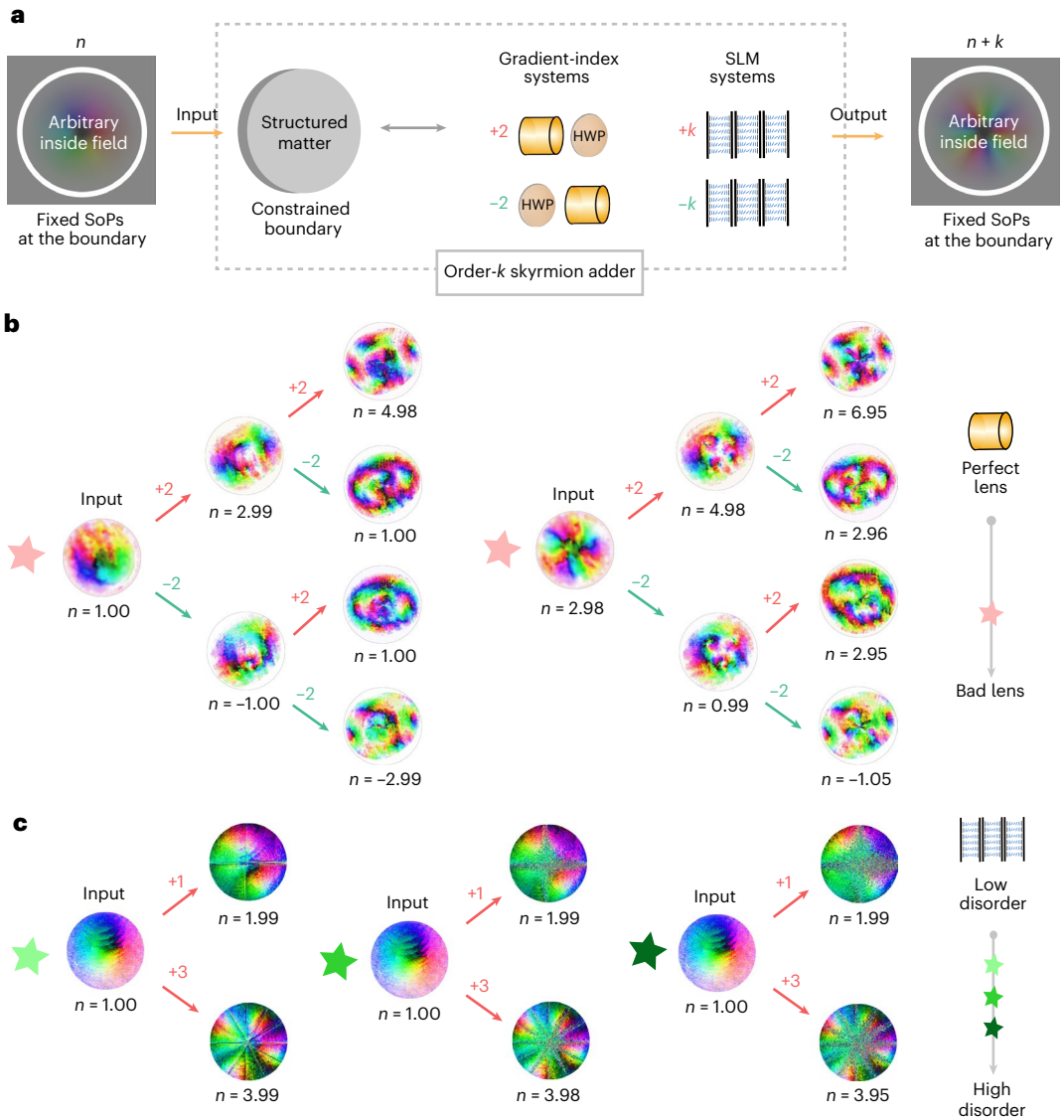

Fig. 2 | Adder modules and experimental results. a, Order-*k* adder modules can be constructed using a linear retarder array placed before a half-wave plate, whereas order-*k* subtractor modules can be constructed using a linear retarder array placed after a half-wave plate. The addition of the half-wave plates resolves incompatibilities in polarization states on the boundary, as explained in the main text, allowing for the different modules to be cascaded indefinitely. Notice also that order-*k* adders and subtractors can be realized using the same hardware, with one direction performing addition and the other performing subtraction. Last, although gradient-index systems and a three-SLM cascade are used to implement the adder in our work, it is worth emphasizing that an adder can be implemented in many different ways, provided its properties at the boundary are properly constrained. **b**, Subset of the measured Stokes fields of optical skyrmions passing through adders of order 2 realized using gradient-index systems. The operations $1 \pm 2 \pm 2$ and $3 \pm 2 \pm 2$ are shown, with the detailed implementation presented in Supplementary Note 1 and the full dataset presented in Supplementary Fig. 2. **c**, Subset of the measured Stokes fields of optical skyrmions passing through adders of orders 1 and 3 realized using a three-SLM cascade, and where disorder is introduced by a random pixel-wise noise to the voltage levels of the SLMs. Since only a single adder is used in this experiment, no half-wave plate is included. Three levels of disorder are shown, as indicated by the colour of the star, increasing from left to right. Details of the implementation are provided in Supplementary Note 1, and a complete dataset is presented in Supplementary Fig. 3.

energy input. Moreover, we demonstrate that by adopting a generalized skyrmion number[42], it is possible to simultaneously increase the dimensionality of information carried and relaxing boundary restrictions. Our work opens the doors to this entirely new framework for performing photonic computing, where optical skyrmions are used as the fundamental unit in computation.

Here we introduce a family of optical skyrmion adders: one for conventional skyrmions and another for generalized skyrmions. Each class of adder functions differently and exhibits a distinct form of topological robustness, which we make precise below. Finally, we discuss the relative strengths and weaknesses of the different adders introduced.

Beginning with conventional skyrmion adders, we provide a mathematical description of our proposed optical component, followed by experimental results that demonstrate its feasibility and robustness to disorder. As detailed in the 'Structured matter design using a general transformation law of skyrmions' section, given a general homotopy of skyrmions, the resulting difference in skyrmion number is equal to the skyrmion number of the homotopy when restricted onto the walls of the homotoping cylinder. This transformation law gives a systematic way of engineering structured matter to perform addition.

For example, consider a spatially varying retarder, which when restricted to its boundary, is linear and has a retardance of π. Let *k* be the number of half-revolutions made by the axis of the retarder traversing

counterclockwise along its boundary (Fig. 1b). Then, with no further restrictions to material properties apart from continuity, one may show

$$\deg \mathcal{S}' = \begin{cases} \deg \mathcal{S}+k & \text{if } \mathcal{S} \text{ is right circularly polarized (RCP) on its boundary} \\ \deg \mathcal{S}-k & \text{if } \mathcal{S} \text{ is left circularly polarized (LCP) on its boundary} \end{cases}, \quad (1)$$

where $\mathcal{S}$ and $\mathcal{S}'$ are the Stokes fields before and after the medium, respectively. We call structured matter satisfying these conditions skyrmion photo-adders of order k.

Our mathematical results also imply that the function of any medium designed in this way depends only on the structure of its boundary and is independent of material properties everywhere else provided they are continuous (excluding certain extreme cases; see the 'Discussion' and 'Structured matter design using a general transformation law of skyrmions' sections). This is a reflection of the topological structure of the optical skyrmion exhibited in matter. From a practical perspective, this suggests a strong robustness of any such adder to physical imperfections of the medium that implements it, which greatly eases fabrication. We demonstrate the robustness arising from this 'topological duality' between field and matter (Fig. 1c), which shows the invariance of the effect of our proposed adder on the skyrmion number of optical fields to perturbations in the medium, and give a more detailed explanation of robustness and duality in the 'Structured matter design using a general transformation law of skyrmions' section.

After passing through the adder proposed above, the boundary conditions of the skyrmion will flip, that is, RCP becomes LCP and vice versa. Therefore, to cascade multiple adders together, one must realign the outer boundary after each operation. With our proposed design, this amounts to adding a half-wave plate after the medium for addition and a half-wave plate before for subtraction, provided we design our components for skyrmions that are RCP on their boundary (Fig. 2a and Supplementary Fig. 6). Therefore, combining an adder with a half-wave plate effectively produces a cascadable module that performs addition in one direction and subtraction in the other.

Next, to demonstrate the feasibility of our proposed medium, we provide experimentally measured Stokes fields of skyrmions passing through second-order adders realized via gradient-index systems. Figure 2b shows a subset of our results, with the full dataset presented in Supplementary Fig. 2. We generated skyrmions of orders ranging from −3 to 3 using a cascade of two spatial light modulators (SLMs) and passed the field through the medium with appropriate wave plates to achieve the operations +2 + 2, +2 − 2, −2 + 2 and −2 − 2 (Supplementary Note 1 provides details of the techniques used in beam generation, measurement and analysis, and Supplementary Fig. 1 shows the experimental assembly). Note that the medium we used was discarded by quality assurance due to its asymmetric axis distribution, and it exhibits substantial perturbations in material properties compared with the typical sample. Despite this, the numerically computed skyrmion numbers show that our proposed adder efficiently and reliably performs the desired operations, even with imperfections in the medium. Further technical details of the experiments are presented in Supplementary Note 1.

To further emphasize the perturbation resilience of our proposed adder and the versatility of its implementation, we present experimental results in which a cascade of three SLMs is used to realize an adder and disorder is simulated by introducing random pixel-wise noise to the voltage levels of the SLMs. Since the three-SLM cascade is designed to achieve arbitrary retardance and axis orientation[8], adding noise to the voltage levels of the SLMs effectively simulates a disordered array of arbitrary elliptical retarders, which has the added benefit of reflecting a wide variety of real-world perturbations. Note that the tunability of SLMs is used to introduce disturbances of varying strengths, but it is not central to how the adder operates (that is, the SLM cascade merely mimics a passive device). The noise is added in such a way that it is the maximum at the centre and gradually decreases to zero at the boundary, consistent with the derivation in the 'Structured matter design using a general transformation law of skyrmions' section. Figure 2c shows a subset of our results with the full dataset, including Mueller matrices of the disordered media and polarization ellipses (Supplementary Fig. 3). This figure shows that the disorder we have added is substantially larger than what would typically occur in practice. Additionally, systematic errors due to phase unwrapping lead to lines observed in the output Stokes field, and this can also be considered a form of perturbation. Nonetheless, the numerically computed skyrmion number remains stable, demonstrating the strong topological robustness of our adder. There remains a large scope for further exploration into the limits of topological protection of optical skyrmions in the presence of random noise, including the effects of spatially correlated noise and the limits at which topological protection breaks down (Supplementary Note 3), which we plan to address in future work.

Last, by adopting the generalized skyrmion number introduced in ref. 42, it is possible to simultaneously enhance the topological robustness of our proposed adder against perturbations in the state of polarization (SoP) of the input light at the boundary, as well as against perturbations in the material parameters at the boundary. Moreover, this approach allows a single field to carry multiple topological charges, representing an increase in the dimensionality of the information carried by the field and greatly improving its information density.

On a more technical level, the generalized skyrmion number is a method of assigning non-compactifiable fields[27] a tuple of integers $(n_1 \ldots n_k)$ derived from the de Rham cohomology of compactly supported forms, which are topologically protected under a general notion of homotopy[42]. Given any smooth polarization field $\mathcal{S} : \Omega \longrightarrow S^2$, we can define one generalized skyrmion number for each connected component of the Poincaré sphere carved out by the image of the boundary curve $\mathcal{S}|_{\partial\Omega}$ (Fig. 3b). The generalized skyrmion number associated with a connected component can be computed by the integral equation

$$\text{Generalized skyrmion number} = \frac{1}{c}\int_{\Omega} f(\mathcal{S})\mathcal{S}\cdot\left(\frac{\partial \mathcal{S}}{\partial x}\times\frac{\partial \mathcal{S}}{\partial y}\right)\mathrm{d}x\mathrm{d}y,$$

where $c = \int_0^{2\pi}\int_0^{\pi} f(\theta,\phi)\sin\theta \mathrm{d}\theta\mathrm{d}\phi$ and f is any smooth real-valued function supported on that component.

Following the line of argument in ref. 42, one has the following: as a skyrmion of degree n propagates within the medium, the image of the boundary curve on the Poincaré sphere transitions from a point to a curve. The generalized skyrmion numbers of the newly generated connected components will then be $n + k$, where k is the number of times the boundary curve encircles each component accounting for orientation, whereas the generalized skyrmion number of the original connected component remains unchanged at n (Fig. 3c shows a single example of this process, with more examples given in Supplementary Fig. 7). Note that the description above also enables the design of arbitrary generalized skyrmion photo-adders, which simultaneously perform an arbitrary number of arbitrary additions, $(n)\mapsto(n + k_1 \ldots n + k_j, n)$ for any number $j \in \mathbb{N}$ and $k_1 \ldots k_j \in \mathbb{Z}$. We describe this in detail in the 'Arbitrary generalized skyrmion adders' section.

Specializing to our proposed adder (whose axis distribution is depicted in Fig. 1b), if the outer retardance is a constant that lies between 0 and π, three cases arise depending on the SoP at the boundary of the incident skyrmion. For SoPs close to RCP, one has the transition $(n)\mapsto(n + k, n)$, for SoPs close to LCP, one has the transition $(n)\mapsto(n - k, n)$, and for all other states, one has the transition $(n)\mapsto(n + k, n - k, n)$. Thus, one can essentially select the adder's function by using different input boundary SoPs.

https://doi.org/10.1038/s41566-025-01779-x

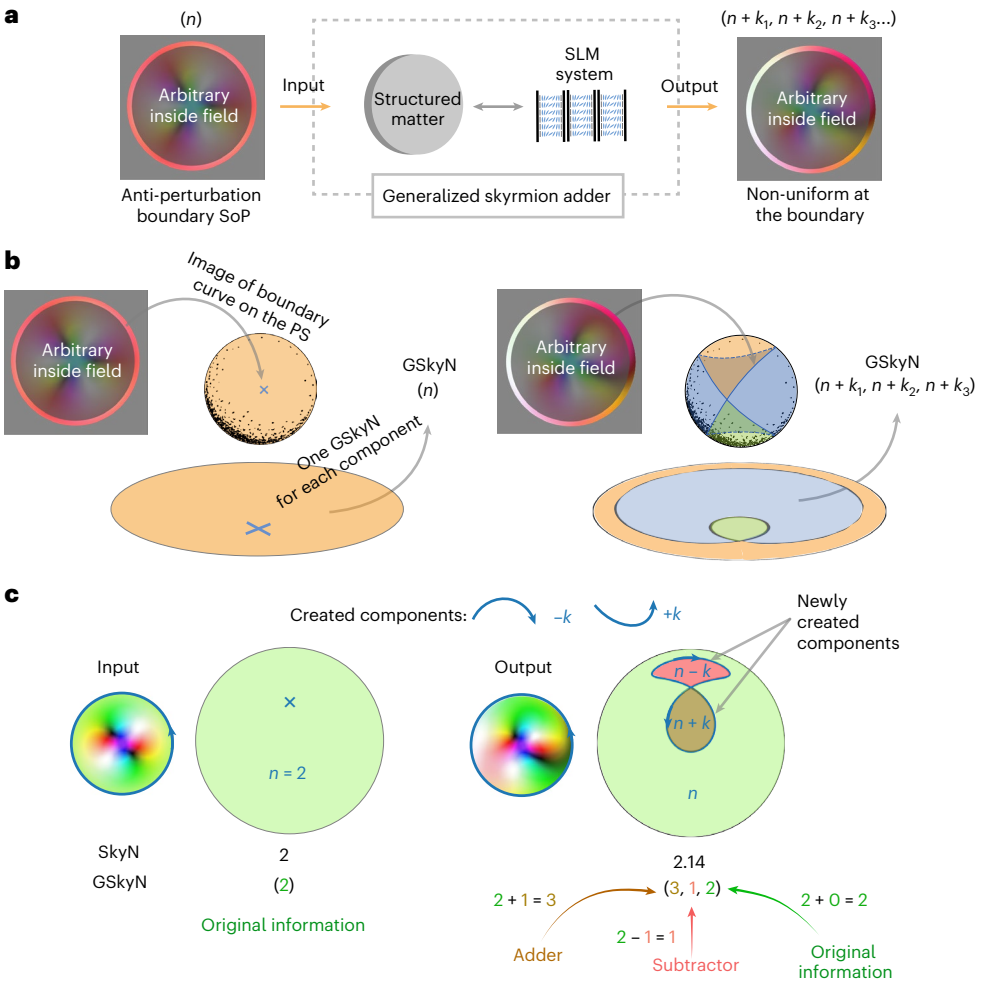

Fig. 3 | Generalized skyrmion adders. a, Concept of a generalized skyrmion photo-adder, which is a passive component that converts a skyrmion of degree n into a generalized skyrmion of degree $(n+k_1, n+k_2, n+k_3...)$. Note that the function of the adder is robust to perturbations in both input field and material parameters, with this robustness extending even to situations in which perturbations occur at the boundary. **b**, Given a polarization field, a single generalized skyrmion number (GSkyN) can be defined for each connected component of the Poincaré sphere carved out by the image of the boundary curve. A field with one component (left) and three components (right), along with the corresponding images of their boundary curves on the Poincaré sphere, is shown. A stereographically projected version of the boundary curve is also shown. Note that for a given boundary condition, any continuous extension of the boundary to the entire domain will have the same number of generalized skyrmion numbers. **c**, A generalized skyrmion adder works by manipulating the boundary to create new connected components. For each newly created component, the original skyrmion number (SkyN) is increased once for each time the boundary curve encircles the component, accounting for orientation. The figure depicts an example of an $(n)\mapsto(n+1, n-1, n)$ adder, with input field $n=2$ and where the Stokes fields and stereographically projected boundary curves are shown. Finally, the skyrmion number and generalized skyrmion numbers of the two fields are provided.

Notice also that by adopting the generalized skyrmion number, not only can we have situations in which multiple additions and subtractions occur simultaneously but there is also a general tolerance to the boundary SoP of the input beam. Indeed, the adder splits the Poincaré sphere into various regions, and performs a specific type of operation on each region. More generally, as long as the number of new connected components that form during propagation and the orientation in which the boundary curve encircles each component remains the same, the same operations will be observed at the level of the generalized skyrmion number. This latter property makes the generalized skyrmion adder stable against fluctuations in the parameters of matter, without the strict constraints at the boundary present in the skyrmion adders introduced earlier. Last, note that although it is possible to manipulate fields with non-integer skyrmion numbers for computation, the skyrmion number in this case is not a topologically protected quantity and, therefore, does not support the same level of robustness as the generalized skyrmion number (Supplementary Note 2).

To demonstrate the powerful robustness of our generalized skyrmion adder, we present the experimental results of uniformly polarized light entering a spatially varying retarder, with the axis configuration shown in Fig. 1b with a single half-revolution and where the outer retardance is π/2. The adder is implemented via a cascade of three SLMs as above, and where disorder is simulated by a random pixel-wise noise to the voltage levels of the SLMs, uniform everywhere including at the boundaries. A two-SLM system that acts as an arbitrary beam generator is separately added (Supplementary Note 1). Figure 4a shows a subset of our results, with a single SoP selected from each region corresponding to addition, subtraction and simultaneous addition and subtraction. A full dataset including details of the incident light, measured Mueller matrices and polarization ellipses is presented in Supplementary Fig. 4. From the computed generalized skyrmion numbers, it is clear that the function of the generalized skyrmion adder is stable with respect to the added disorder.

Moreover, in the full dataset presented in Supplementary Fig. 4, we demonstrate that the function of the adder is stable within a range

https://doi.org/10.1038/s41566-025-01779-x

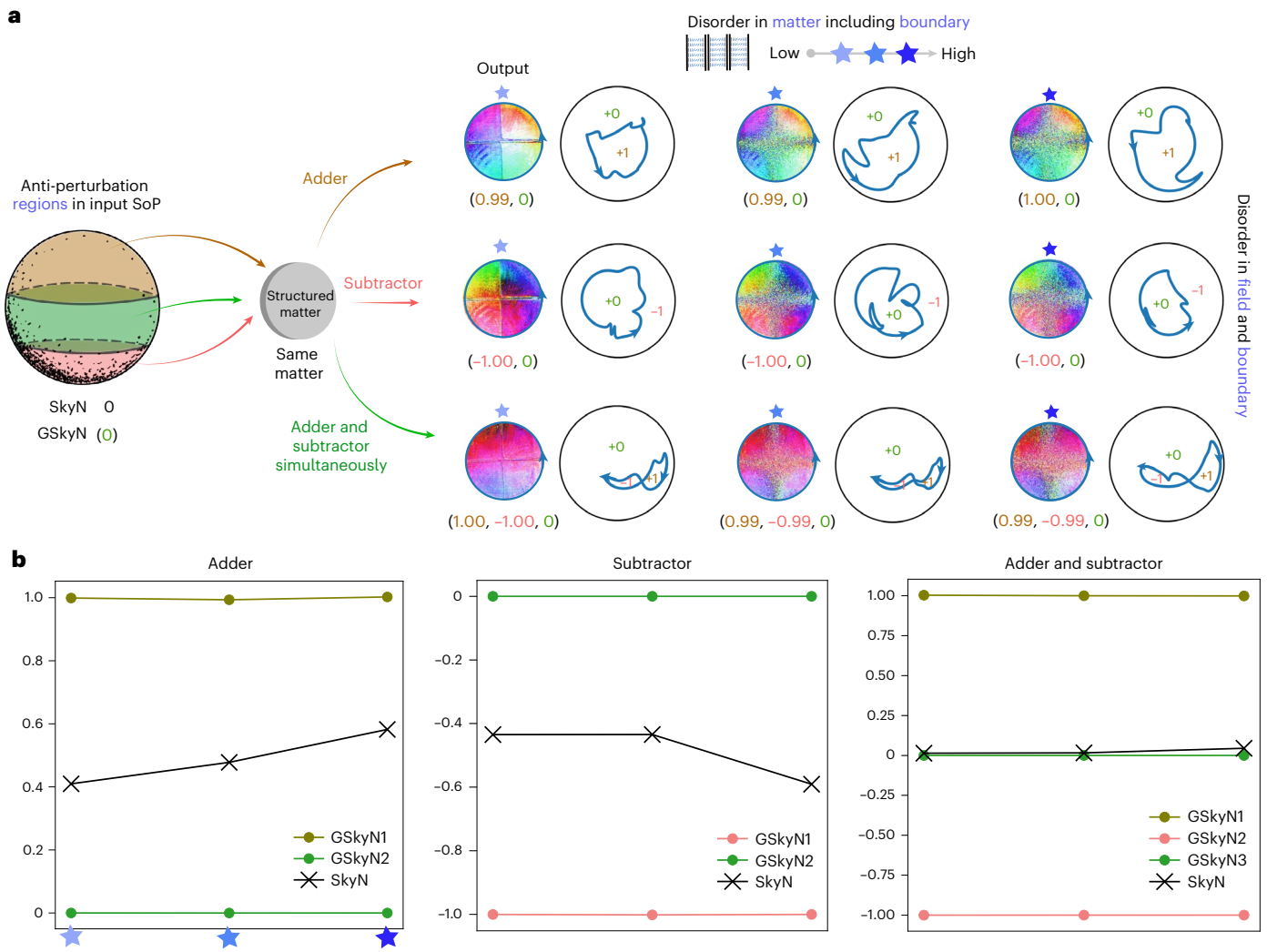

Fig. 4 | Experimental results (generalized skyrmion adders). a, (Left) The different regions of the Poincaré sphere on which the function of our adder is stable. The top region corresponds to addition; the bottom, to subtraction; and the middle, to both addition and subtraction simultaneously. (Right) A subset of the measured output Stokes fields and computed generalized skyrmion numbers is shown for different levels of disorder (increasing from left to right) and different incident SoPs selected to demonstrate addition, subtraction and simultaneous addition and subtraction. A stereographic projection of the boundary curve is also shown, with the change in skyrmion number of each region labelled. The colour of these labels indicate the generalized skyrmion number corresponding to that region. A complete dataset including details of the incident SoPs and measured Mueller matrices is presented in Supplementary Fig. 4. Technical details such as the formation of small loops due to disorder are also discussed. Last, details of the implementation and experimental assembly are provided in Supplementary Note 1 and Supplementary Fig. 1, respectively. **b**, Skyrmion number and generalized skyrmion numbers at each level of disorder for different incident SoPs. Note that the generalized skyrmion number is topologically stable even though the usual skyrmion number is not.

of SoPs. This stability of the generalized skyrmion adder to different inputs is an important feature, which is not enjoyed by the skyrmion adders introduced earlier. Last, a comparison between the skyrmion number and generalized skyrmion numbers at different levels of disorders is also shown in Fig. 4b. From the plots, it is clear that the generalized skyrmion number is topologically stable even though the usual skyrmion number is not. The technique of computing the generalized skyrmion number and estimating the boundary curve is adapted from ref. 42.

A more detailed analysis of the experimental results is presented in Supplementary Note 1.4, including discussions on topological protection and engineering solutions for the formation of small loops in the boundary due to disorder.

In summary, adopting the generalized skyrmion number offers many advantages. Not only are there straightforward methods for creating generalized skyrmion photo-adders capable of performing an arbitrary number of arbitrary integer additions simultaneously but these systems also exhibit strong robustness against perturbations in both the incident field and the material implementing the adder, with weaker boundary restrictions.

There are, however, limitations to using the generalized skyrmion number as well, such as difficulties in retrieving the generalized skyrmion number from polarimetric measurements. Our proposed design also only allows for the conversion of a regular skyrmion to a generalized skyrmion and is, therefore, not immediately cascadable. In the 'Arbitrary generalized skyrmion adders' section, a rudimentary strategy for cascading generalized adders is introduced. Last, we note that there remains room to explore strategies for directly converting generalized skyrmions to other generalized skyrmions in the context of optical computing. Given its discrete nature, topological robustness and high dimensionality, we believe that the manipulation of generalized skyrmions represents a real and meaningful advancement in the use of optical skyrmions for high-density data applications that extend beyond computing.

Discussion

In this paper, we have demonstrated a method of achieving digital computing with optical skyrmions using structured matter. In practice, adders of arbitrary orders can be fabricated through numerous techniques including the laser polymerization of liquid crystals[43,44], metasurfaces[45–49], gradient-index systems, SLM cascades[8], direct laser writing of birefringent structures in silica[50,51], inkjet printing of liquid crystal droplets[52], compact meta-fibres[53] and more, all of which suggest the possibility of manufacturing compact microscale devices containing such adders.

As mentioned earlier, a crucial property of both proposed skyrmion photo-adders is that its effect on skyrmion fields depends only on the structure of their boundary, a reflection of the topological nature of the optical skyrmion. From an engineering perspective, this provides clear advantages in manufacturing as the tolerable margins of error in fabrication are greatly relaxed, with no further restrictions on the medium besides the continuity of its material properties. In particular, the function of the adder is independent of perturbations to material properties away from the boundary, including spatially varying anisotropic absorptions with tolerance up to a certain diattenuation and complex spatially varying retardance such as those resulting from birefringence (see the 'Structured matter design using a general transformation law of skyrmions' section and ref. 27 for more details). Moreover, these conditions can be further relaxed if the framework of the generalized skyrmion number is adopted.

Despite the numerous promising properties of skyrmions for photonic computing, achieving full skyrmion-based computing still requires solutions to many important problems in manufacturing, architecture and on-chip integration. Here we outline the possible solutions to some of the hurdles that may arise.

First, understanding the non-trivial behaviour of polarization fields in waveguides is of key importance for enabling small integrated devices to make use of skyrmions. In particular, apart from fabricating the adders themselves, it is also necessary to relay polarization information between adders for any meaningful computation to be done. For a waveguide to support the propagation of complex structured fields, it must necessarily be large enough to carry multiple modes. Moreover, work will need to be done to establish the range of skyrmion numbers that can be achieved by an arbitrary superposition of propagating modes and the conservation of skyrmion number in propagation. Here we provide a heuristic argument suggesting the feasibility of topological protection. On the basis of the ellipticity of the Helmholtz equation, in general, the electric field develops continuously within the waveguide. This then naturally descends onto a homotopy of Stokes fields provided there are no zeros in the field. Therefore, at least for some finite distance, we expect the skyrmion number to remain unchanged[54], supporting potential use in optical interconnects, where communication typically occurs over short, chip-scale distances.

Second, although our proposed medium theoretically supports wavelength-division multiplexing, the generally wavelength-dependent nature of retarders may limit the number of independent operations that can be carried out simultaneously. Nevertheless, with the improving quality of on-chip comb lasers[55] and broadband retarders implemented through metamaterials[45–48], such limitations are perhaps more a matter of engineering.

Third, besides considerations relating to the medium, any system exploiting skyrmions will also require auxiliary support for generating and detecting skyrmions. With regard to generation[56], notice that uniform polarized light is trivially a skyrmion of degree 0. Therefore, our proposed medium can create optical skyrmions, where incident RCP and LCP light generate skyrmions of degree $+k$ and $-k$, respectively. Regarding detection, recent developments in on-chip Stokes polarimetry[57] support the possibility of accurately measuring complex polarization fields on integrated circuits. However, extracting the topological number from polarimetric measurements should be done efficiently for a skyrmion-based photonic adder to be feasible. Note that apart from evaluating the skyrmion number integral, various other properties of the topological number can be used to determine the skyrmion number such as counting strategies involving regular values[27]. An alternative way of detection is to exploit light–matter interactions modulated by skyrmions, such as through optomechanical interactions between optical skyrmions and topological solitons in liquid crystals[58].

Last, depending on implementation, both passive and tunable adders can be fabricated. The best implementation will ultimately depend on the application, with tunable elements providing greater flexibility at the cost of greater power consumption, possible hysteresis and greater complexity in control. We reiterate that in our work, we use SLMs to mimic a passive retarder array with disorder, rather than taking advantage of their tunability.

Despite the challenges presented above, we believe that photonic computing using optical skyrmions remains an exciting avenue to explore. Given the rise of artificial intelligence and machine learning, the need for power-efficient computing technologies is more important than ever. Photonic computing has emerged as a promising solution to meet this need, and optical skyrmions represent a way of carrying high-dimensional information within optical fields that holds great potential for enhancing information density in photonic computing without additional energy cost. With wavelength, amplitude and phase information (including structured phase) accessible independent of spatially varying polarization and, hence, any underlying skyrmion structure, there are certainly intriguing prospects for combining different existing architectures to exploit all these dimensions simultaneously.

Moreover, our work provides a method of directly exploiting the topological and discrete nature of the skyrmion for computations and, therefore, a route to create robust digital photonic computing tolerant to perturbations and noise with strong potential for scalability. This is particularly so with our introduction of the generalized skyrmion number, which enables the transmission of multiple independent topologically protected quantities within a single field—including those with singularities, which, in effect, behave as additional boundaries that can be manipulated—allowing for spatial-domain multiplexing in an entirely novel way. We believe this makes our proposed approach one of the most promising strategies for increasing the number of TOPS (trillions (10^{12}) of operations per second, or tera-ops per second) in modern photonic processors. Most importantly, using optical skyrmions as units of computation expands the traditional notion of the bit to theoretically infinite values and, therefore, has the potential to alter the binary foundations of digital computing fundamentally.

As a concluding remark, we note that with addition and subtraction possible, the remaining mathematical operations become a matter of design (Supplementary Note 4). However, skyrmions also support a more natural notion of multiplication. Suppose a homogeneous medium induces a mapping on the Poincaré sphere of degree k. The effect of such a medium on skyrmions is equivalent to multiplication by k, with no other restrictions on the input field. For example, a medium whose action on the Poincaré sphere is given by

$$(\sin\phi\cos\theta, \sin\phi\sin\theta, \cos\phi) \mapsto (\sin\phi\cos k\theta, \sin\phi\sin k\theta, \cos\phi)$$

is a skyrmion multiplier of order k, whereas a mirror can be regarded as a multiplier of order -1 with the proper choice of coordinates[59]. Last, if such a multiplier can be implemented, then division is naturally also possible. One way to achieve this is by taking the unique advantage of the fact that skyrmions are integer valued and not limited to 0 and 1 like bits in conventional digital electronics. This property enables the use of more novel fundamental units of data; for example, a single rational number can be represented by either two conventional skyrmions or a single generalized skyrmion $p/q \Leftrightarrow (p, q)$.

Addition, multiplication and division can then be implemented by $(p_1, q_1) + (p_2, q_2) = (p_1q_2 + p_2q_1, q_1q_2)$, $(p_1, q_1) \times (p_2, q_2) = (p_1p_2, q_1q_2)$ and $(p_1, q_1) \div (p_2, q_2) = (p_1q_2, p_2q_1)$, respectively.

Online content

Any methods, additional references, Nature Portfolio reporting summaries, source data, extended data, supplementary information, acknowledgements, peer review information; details of author contributions and competing interests; and statements of data and code availability are available at https://doi.org/10.1038/s41566-025-01779-x.

References

1. Tsesses, S. et al. Optical skyrmion lattice in evanescent electromagnetic fields. *Science* **361**, 993–996 (2018).
2. He, C., Shen, Y. J. & Forbes, A. Towards higher-dimensional structured light. *Light Sci. Appl.* **11**, 205 (2022).
3. Sugic, D. et al. Particle-like topologies in light. *Nat. Commun.* **12**, 6785 (2021).
4. Shen, Y. J., Martínez, E. C. & Rosales-Guzmán, C. Generation of optical skyrmions with tunable topological textures. *ACS Photonics* **9**, 296–303 (2022).
5. Bai, C. Y. et al. Dynamic tailoring of an optical skyrmion lattice in surface plasmon polaritons. *Opt. Express* **28**, 10320–10328 (2020).
6. Lin, W. B. et al. Microcavity-based generation of full Poincaré beams with arbitrary skyrmion numbers. *Phys. Rev. Res.* **3**, 023055 (2021).
7. Cisowski, C., Ross, C. & Franke-Arnold, S. Building paraxial optical skyrmions using rational maps. *Adv. Photonics Res.* **4**, 2200350 (2023).
8. He, C. et al. A reconfigurable arbitrary retarder array as complex structured matter. *Nat. Commun.* **16**, 4902 (2025).
9. Du, L. P. et al. Deep-subwavelength features of photonic skyrmions in a confined electromagnetic field with orbital angular momentum. *Nat. Phys.* **15**, 650–654 (2019).
10. Lei, X. R. et al. Photonic spin lattices: symmetry constraints for skyrmion and meron topologies. *Phys. Rev. Lett.* **127**, 237403 (2021).
11. Shi, P., Du, L. P. & Yuan, X. C. Strong spin–orbit interaction of photonic skyrmions at the general optical interface. *Nanophotonics* **9**, 4619–4628 (2020).
12. Teng, H. A. et al. Physical conversion and superposition of optical skyrmion topologies. *Photon. Res.* **11**, 2042–2053 (2023).
13. Shen, Y. J. et al. Optical skyrmions and other topological quasiparticles of light. *Nat. Photon.* **18**, 15–25 (2024).
14. Shen, Y. J. et al. Supertoroidal light pulses as electromagnetic skyrmions propagating in free space. *Nat. Commun.* **12**, 5891 (2021).
15. Gao, S. J. et al. Paraxial skyrmionic beams. *Phys. Rev. A* **102**, 053513 (2020).
16. Ma, J. et al. Nanophotonic quantum skyrmions enabled by semiconductor cavity quantum electrodynamics. *Nat. Phys.* **21**, 1462–1468 (2025).
17. Zeng, X. J. et al. Tailoring ultra-high-order optical skyrmions. *Laser Photonics Rev.* **19**, e00732 (2025).
18. Wang, J. W. et al. Generation of ring-shaped optical skyrmion with a high topological number. *Appl. Phys. Lett.* **126**, 201103 (2025).
19. Shen, Y. J., Wang, H. W. & Fan, S. H. Free-space topological optical textures: tutorial. *Adv. Opt. Photon.* **17**, 295–374 (2025).
20. Shen, Y. J. Topological light waves: skyrmions can fly. *Optics Photon. News* **36**, 26–33 (2025).
21. Nagaosa, N. & Tokura, Y. Topological properties and dynamics of magnetic skyrmions. *Nat. Nanotechnol.* **8**, 899–911 (2013).
22. Je, S. G. et al. Direct demonstration of topological stability of magnetic skyrmions via topology manipulation. *ACS Nano* **14**, 3251–3258 (2020).
23. Cortés-Ortuño, D. et al. Thermal stability and topological protection of skyrmions in nanotracks. *Sci. Rep.* **7**, 4060 (2017).
24. Ornelas, P. et al. Non-local skyrmions as topologically resilient quantum entangled states of light. *Nat. Photon.* **18**, 258–266 (2024).
25. Ornelas, P. et al. Topological rejection of noise by quantum skyrmions. *Nat. Commun.* **16**, 2934 (2025).
26. Liu, C. X. et al. Disorder-induced topological state transition in the optical skyrmion family. *Phys. Rev. Lett.* **129**, 267401 (2022).
27. Wang, A. A. et al. Topological protection of optical skyrmions through complex media. *Light Sci. Appl.* **13**, 314 (2024).
28. Shen, Y. C. et al. Deep learning with coherent nanophotonic circuits. *Nat. Photon.* **11**, 441–446 (2017).
29. Shokraneh, F., Geoffroy-Gagnon, S., Nezami, M. S. & Liboiron-Ladouceur, O. A single layer neural network implemented by a 4 x 4 MZI-based optical processor. *IEEE Photon.* **11**, 4501612 (2019).
30. Tait, A. N. et al. Neuromorphic photonic networks using silicon photonic weight banks. *Sci. Rep.* **7**, 7430 (2017).
31. Tait, A. N. et al. Microring weight banks. *IEEE J. Sel. Topics Quantum Electron.* **22**, 312–325 (2016).
32. Feldmann, J. et al. Parallel convolutional processing using an integrated photonic tensor core. *Nature* **589**, 52–58 (2021).
33. Zhou, W. et al. In-memory photonic dot-product engine with electrically programmable weight banks. *Nat. Commun.* **14**, 2887 (2023).
34. Song, L. J., Li, H. & Dai, D. Mach–Zehnder silicon-photonic switch with low random phase errors. *Opt. Lett.* **46**, 78–81 (2021).
35. Huang, C. R. et al. Demonstration of scalable microring weight bank control for large-scale photonic integrated circuits. *APL Photonics* **5**, 040803 (2020).
36. Komljenovic, T. & Pintus, P. On-chip calibration and control of optical phased arrays. *Opt. Express* **26**, 3199–3210 (2018).
37. Ahmed, S. R. et al. Universal photonic artificial intelligence acceleration. *Nature* **640**, 368–374 (2025).
38. Hua, S. Y. et al. An integrated large-scale photonic accelerator with ultralow latency. *Nature* **640**, 361–367 (2025).
39. Fang, X. Y. et al. Orbital angular momentum-mediated machine learning for high-accuracy mode-feature encoding. *Light Sci. Appl.* **13**, 49 (2024).
40. Hong, L. et al. Experimental optical computing of complex vector convolution with twisted light. *Adv. Photon. Nexus* **2**, 046008 (2023).
41. Zhang, K. et al. Advanced all-optical classification using orbital–angular–momentum–encoded diffractive networks. *Adv. Photon. Nexus* **2**, 066006 (2023).
42. Wang, A. A. et al. Generalized skyrmions. Preprint at https://arxiv.org/abs/2409.17390 (2024).
43. Zeng, H. et al. High-resolution 3D direct laser writing for liquid-crystalline elastomer microstructures. *Adv. Mater.* **26**, 2319–2322 (2014).
44. Tartan, C. C. et al. Read on demand images in laser-written polymerizable liquid crystal devices. *Adv. Opt. Mater.* **6**, 1800515 (2018).
45. Yu, N. F. et al. A broadband, background-free quarter-wave plate based on plasmonic metasurfaces. *Nano Lett.* **12**, 6328–6333 (2012).
46. Khorasaninejad, M. et al. Broadband and chiral binary dielectric meta-holograms. *Sci. Adv.* **2**, e1501258 (2016).
47. Devlin, R. C. et al. Broadband high-efficiency dielectric metasurfaces for the visible spectrum. *Proc. Natl Acad. Sci. USA* **113**, 10473–10478 (2016).
48. Wen, D. D. et al. Helicity multiplexed broadband metasurface holograms. *Nat. Commun.* **6**, 8241 (2015).
49. Yu, N. J. et al. Light propagation with phase discontinuities: generalized laws of reflection and refraction. *Science* **334**, 333–337 (2011).

50. Fedotov, S. S. et al. Direct writing of birefringent elements by ultrafast laser nanostructuring in multicomponent glass. *Appl. Phys. Lett.* **108**, 071905 (2016).
51. Bricchi, E., Klappauf, B. G. & Kazansky, P. G. Form birefringence and negative index change created by femtosecond direct writing in transparent materials. *Opt. Lett.* **29**, 119–121 (2004).
52. Kamal, W. et al. On-demand pitch tuning of printed chiral nematic liquid crystal droplets. *Mater. Today Adv.* **19**, 100416 (2023).
53. He, T. T. et al. Optical skyrmions from metafibers with subwavelength features. *Nat. Commun.* **15**, 10141 (2024).
54. Wang, A. A. et al. Optical skyrmions in waveguides. Preprint at https://arxiv.org/abs/2505.06735 (2025).
55. Gaeta, A. L., Lipson, M. & Kippenberg, T. J. Photonic-chip-based frequency combs. *Nat. Photon.* **13**, 158–169 (2019).
56. Lin, W. B. et al. On-chip optical skyrmionic beam generators. *Optica* **11**, 1588–1594 (2024).
57. Zuo, J. W. et al. Chip-integrated metasurface full-Stokes polarimetric imaging sensor. *Light Sci. Appl.* **12**, 218 (2023).
58. Poy, G. et al. Interaction and co-assembly of optical and topological solitons. *Nat. Photon.* **16**, 454–461 (2022).
59. Chen, J., Forbes, A. & Qiu, C. W. More than just a name? From magnetic to optical skyrmions and the topology of light. *Light Sci. Appl.* **14**, 28 (2025).

Methods

Structured matter design using a general transformation law of skyrmions

Here we derive a general transformation law of skyrmions from which we can observe a powerful heuristic of topological duality, namely, changes to the skyrmion number induced by a medium depend primarily on the structure of the medium on its boundary. As we will explain, this notion of duality has important implications for the design of structured matter to manipulate the skyrmion number, providing a strong tolerance to perturbations of material parameters away from the boundary.

As an aside, in this paper, we use the term structured matter as an umbrella term for the different types of matter that are used to generate and manipulate structured light[8,27]. Typically, these are complex spatially varying media that can precisely modulate the phase, polarization and intensity of light, and can be abstractly described using Jones or Mueller calculus. Important classes of structured matter include spatially varying retarders, diattenuators and depolarizers[60]. This framework of structured matter enables the abstract design of complex components, which can then be implemented using different technologies (including metasurfaces, liquid crystal devices and various other examples mentioned in this paper) tailored to practical requirements such as size, resolution, tunability, reconfigurability, dynamic control, rewritability (for example, for information storage) and more[61–63]. Additionally, the topological properties of structured matter remain a largely unexplored area with potential applications in beam generation and analysis, biomedical imaging, communications, information storage and, as demonstrated in this paper, computing.

In the following, we denote by $B_a(0)$ the ball of radius a centred at the origin. Let $\mathcal{S}, \mathcal{S}' : \overline{B_a(0)} \longrightarrow S^2$ be two different continuous polarization fields that are constant on the boundary. $\mathcal{S}$ and $\mathcal{S}'$ then descend onto the quotient $\overline{B_a(0)}/\sim \cong S^2$ obtained by identifying points on $\partial B_a(0)$ and are, therefore, skyrmions.

Suppose we can find a continuous homotopy $F : \overline{B_a(0)} \times [0,1] \longrightarrow S^2$ from $\mathcal{S}$ to $\mathcal{S}'$. Let $S^+ = \{(s^1, s^2, s^3) \in S^2 : s^3 \geq 0\}$ and $S^- = \{(s^1, s^2, s^3) \in S^2 : s^3 \leq 0\}$ denote the northern and southern hemispheres, respectively, and define $\psi_+ : B_a(0) \to S^+$

$$\psi_+(r\cos\theta, r\sin\theta) = \left(\sqrt{1-(r/a)^2}\cos\theta, \sqrt{1-(r/a)^2}\sin\theta, \sqrt{1-(r/a)^2}\right)$$

and $\psi_- : \overline{B_a(0)} \longrightarrow S^-$,

$$\psi_-(r\cos\theta, r\sin\theta) = \left(\sqrt{1-(r/a)^2}\cos\theta, \sqrt{1-(r/a)^2}\sin\theta, -\sqrt{1-(r/a)^2}\right)$$

so that ψ_+ is an orientation-preserving diffeomorphism onto its image and ψ_- is an orientation-reversing diffeomorphism onto its image. Now, let $H: S^2 \times [0,1] \to S^2$ be

$$H(s,z) = \begin{cases} F(\psi_+^{-1}(s), z), & s \in \overline{S^+} \\ F(a\cos\theta, a\sin\theta, z(1+s_3)), & s \in \overline{S^-} \end{cases},$$

where $s = (s_1, s_2, s_3) = (\sin\phi\cos\theta, \sin\phi\sin\theta, \cos\phi) \in S^2$. Then, H is a continuous by a gluing argument, and by the homotopy invariance of the degree, we have $\deg H(\cdot, 0) = \deg H(\cdot, 1)$.

It is clear that $\deg H(\cdot, 0) = \deg \mathcal{S}$ and $\deg H(\cdot, 1) = \deg \mathcal{S}' + \deg \partial F$, where $\partial F : \partial B_a(0) \times [0,1]/\sim \cong S^2 \longrightarrow S^2$ with the identifications $(x, 0) \sim (y, 0)$ and $(x, 1) \sim (y, 1)$ for all $x, y \in \partial B_a(0)$ and $\partial F([x]) = F(\iota(x))$ for the trivial inclusion $\iota : \partial B_a(0) \times [0,1] \longrightarrow \overline{B_a(0)} \times [0,1]$. Therefore,

$$\deg \mathcal{S} = \deg \mathcal{S}' + \deg \partial F.$$

If, further, ∂F is C^1, we have the integral equation

$$\deg \mathcal{S} = \deg \mathcal{S}' + \int_{S^2} (\partial F)^* \omega$$

for every normalized $\omega \in \Lambda^2(S^2)$.

In particular, this proves that given a general homotopy of skyrmions, the resulting difference in skyrmion number is equal to the skyrmion number of the homotopy when restricted onto the walls of the homotoping cylinder. To make this statement more intuitive, consider the polarization field as it propagates through the medium. Initially, the boundary of the field is a single point on the Poincaré sphere. However, as the field propagates, its boundary need not remain constant valued, but instead, traces out a curve on the Poincaré sphere. Last, this curve collapses back into a point at the output. This situation is, therefore, exactly analogous to the 'unwrapping' of the Poincaré sphere from the north pole to the south pole that is usually used to describe the skyrmion (except here we allow for the unwrapping between two arbitrary SoPs), and indeed, the number of times the Poincaré sphere is unwrapped is exactly the difference in the skyrmion numbers of the input and output fields.

From the argument above, it is easy to understand why our proposed adder exhibits resilience to perturbations away from the boundary. This resilience arises because the change in skyrmion number depends solely on how the polarization states at the boundary are 'unwrapped,' which, in turn, depends only on the material parameters at the boundary. In this sense, there is a 'duality' between light and matter, in which specifying the boundary condition of one imposes a corresponding condition on the other.

Another way to understand topological robustness is through the theory presented in ref. 27, which provides precise conditions for the topological protection of optical skyrmions across a wide range of media, including spatially varying retarders, diattenuators, depolarizers and cascades of these elements. By considering the Jones or Mueller matrix of a real adder as a composition of an ideal adder and a matrix encoding the non-idealities, the theory in ref. 27 can be applied directly to this additional matrix.

With the procedure developed above, we may prove the following. Consider a continuous spatially varying elliptical retarder $J : \overline{B_a(0)} \longrightarrow \mathrm{SU}(2)$ given by the parameterization

$$J(\alpha, \delta, \Delta) = \begin{pmatrix} \cos^2(\alpha)e^{i\Delta/2} + \sin^2(\alpha)e^{-i\Delta/2} & 2i\cos(\alpha)\sin(\alpha)\sin(\Delta/2)e^{-i\delta} \\ 2i\cos(\alpha)\sin(\alpha)\sin(\Delta/2)e^{i\delta} & \sin^2(\alpha)e^{i\Delta/2} + \cos^2(\alpha)e^{-i\Delta/2} \end{pmatrix},$$

where $\mathcal{Q} \circ \alpha : \overline{B_a(0)} \longrightarrow \mathbb{RP}^1 = \mathbb{R}/(x \sim x + \pi)$ and $\mathcal{P} \circ \delta : \overline{B_a(0)} \longrightarrow S^1 = \mathbb{R}/(x \sim x + 2\pi)$ are continuous maps defining a continuously varying fast axis $(\cos(\alpha)e^{-i\delta/2}, \sin(\alpha)e^{i\delta/2})$, $\mathcal{Q}$ and $\mathcal{P}$ are the respective quotient maps, and $\mathcal{P} \circ \Delta : \overline{B_a(0)} \longrightarrow S^1$ is the corresponding continuously varying retardance. Then, the output field $\mathcal{S}'$ is given by

$$\mathcal{S}'(x) = A^{\mathrm{T}}\mathrm{Spin}\left(J(\alpha(x), \delta(x), \Delta(x))\right)A\mathcal{S}(x),$$

where Spin: SU(2)→SO(3) is the usual Spin map

$$\begin{pmatrix} a+bi & c+di \\ -c+di & a-bi \end{pmatrix} \mapsto \begin{pmatrix} a^2-b^2-c^2+d^2 & 2ab+2cd & -2ac+2bd \\ -2ab+2cd & a^2-b^2+c^2-d^2 & 2ad+2bc \\ 2ac+2bd & 2bc-2ad & a^2+b^2-c^2-d^2 \end{pmatrix}$$

and

$$A = \begin{pmatrix} 0 & 1 & 0 \\ 0 & 0 & 1 \\ 1 & 0 & 0 \end{pmatrix}.$$

Suppose now that $\mathcal{P} \circ \delta|_{\partial B_a(0)} = [0]$ and $\mathcal{P} \circ \Delta|_{\partial B_a(0)} = [\pi]$. If we further restrict to inputs that satisfy $\mathcal{S}|_{\partial B_a(0)} = (0,0,1)^{\mathrm{T}}$, then $\mathcal{S}'$ satisfies

$\mathcal{S}'|_{\partial B_a(0)} = (0,0,-1)^{\mathrm{T}}$ and is, therefore, a skyrmion. Moreover, we may homotope $\mathcal{S}$ to $\mathcal{S}'$ by

$$F(x,z) = A^{\mathrm{T}}\mathrm{Spin}(J(\alpha(x),\delta(x),\Delta(x)z))A\mathcal{S}(x).$$

One can then directly compute

$$\partial F([\theta,z]) = \begin{pmatrix} -\sin(2\partial\alpha(\theta))\sin((2n+1)\pi z) \\ \cos(2\partial\alpha(\theta))\sin((2n+1)\pi z) \\ \cos((2n+1)\pi z) \end{pmatrix}$$

for some integer $n \in \mathbb{Z}$ and where $\partial\alpha := \alpha|_{\partial B_a(0)}$. Taking $\omega \in \Lambda^2(S^2)$ to be the standard volume form on S^2 and assuming sufficient smoothness, we have

$$\begin{aligned}
\deg \partial F &= \int_{S^2} (\partial F)^* \omega \\
&= \int_0^{2\pi}\int_0^1 \frac{1}{4\pi}\partial F \cdot (\partial F_\theta \times \partial F_z)\,\mathrm{d}z\mathrm{d}\theta \\
&= \int_0^{2\pi}\int_0^1 -\frac{2n+1}{2}\sin((2n+1)\pi z)\frac{\mathrm{d}\partial\alpha}{\mathrm{d}\theta}\mathrm{d}z\mathrm{d}\theta \\
&= -\frac{1}{\pi}\int_0^{2\pi}\frac{\mathrm{d}\partial\alpha}{\mathrm{d}\theta}\mathrm{d}\theta \\
&= -\deg \mathcal{Q}\circ\partial\alpha
\end{aligned}$$

where ∂F_θ and ∂F_z are partial derivatives of ∂F with respect to θ and z, respectively. Therefore,

$$\deg \mathcal{S}' = \deg \mathcal{S} + \deg \mathcal{Q}\circ\partial\alpha$$

depends only on the number of revolutions made by the fast axis along the boundary of the medium. An identical proof can be used in the $\partial\mathcal{S}|_{\partial B_a(0)} = (0,0,-1)^{\mathrm{T}}$ case to show

$$\deg \mathcal{S}' = \deg \mathcal{S} - \deg \mathcal{Q}\circ\partial\alpha.$$

Last, note that although other works[64–66] have investigated similar-structured linear retarder arrays for skyrmion generation, our study focuses on a broader class of structured matter (including spatially varying elliptical retarder arrays) and demonstrates the topological properties of such media and their ability to modify the topological number of non-uniform input fields.

Arbitrary generalized skyrmion adders

Here we describe steps to design an arbitrary generalized skyrmion adder that performs the operation $(n)\mapsto(n+k_1 \ldots n+k_j, n)$ for any collection $k_1 \ldots k_j \in \mathbb{Z}$ using elliptical retarders.

1. Pick an incident boundary SoP with Jones vector $J = (J_1, J_2)^{\mathrm{T}} \in \mathbb{C}^2$.
2. Design a smooth curve on the Poincaré sphere that carves out j components so that the curve encircles the ith component k_i times accounting for orientation.
3. Lift the curve from Stokes parameters to Jones vectors.
4. Suppose we are working with a circular domain $B_a(0)$. Let $(\gamma_1,\gamma_2) \in \mathbb{C}^2$ be the curve obtained in step 3, and set

$$\Gamma(\theta) = \begin{pmatrix} \gamma_1(\theta) & -\bar{\gamma}_2(\theta) \\ \gamma_2(\theta) & \bar{\gamma}_1(\theta) \end{pmatrix}\begin{pmatrix} J_1 & -\bar{J}_2 \\ J_2 & \bar{J}_1 \end{pmatrix}^{\dagger} \in \mathrm{SU}(2),$$

where † represents the conjugate transpose. Notice that $\Gamma(\theta)J = (\gamma_1(\theta), \gamma_2(\theta))$ by construction. Thus, we need only extend Γ to all of $B_a(0)$.

5. Let $\Phi : \mathrm{SU}(2) \longrightarrow S^3$ be the canonical diffeomorphism

$$\Phi\begin{pmatrix} a+b\mathrm{i} & -c+d\mathrm{i} \\ c+d\mathrm{i} & a-b\mathrm{i} \end{pmatrix} = \begin{pmatrix} a \\ b \\ c \\ d \end{pmatrix}.$$

We define $\tilde{\Gamma} : B_a(0) \longrightarrow \mathrm{SU}(2)$ by

$$\Phi(\tilde{\Gamma}(r,\theta)) = \frac{(r/a)\Phi(\Gamma(\theta)) + (1-r/a)p}{\left\|(r/a)\Phi(\Gamma(\theta)) + (1-r/a)p\right\|},$$

where $-p$ is any point not in the image of $\Phi\circ\Gamma$.

The function $\tilde{\Gamma}$ from the procedure above describes a spatially varying Jones matrix that performs the desired additions. However, it is worth noting that the higher the order of the adder and the greater the number of numbers added simultaneously, the more challenging it becomes to realize these adders in practice. Nonetheless, we believe there is great potential to further explore such adders and to develop adders capable of converting between generalized skyrmions.

As a side note, a generalized skyrmion can be converted back into an ordinary skyrmion using a diattenuator with fixed axes and a spatially varying extinction ratio that approaches infinity at its boundary. In this case, the resultant skyrmion number corresponds to the connected component containing the state parallel to the diattenuator's transmissive axis. This then allows for different generalized adders to be cascaded.

Data availability

All the main data supporting the results of this study are available within the Article and its Supplementary Information. The data that support the plots within this paper and other findings of this study are available from the corresponding authors upon reasonable request. Source data are provided with this paper.

References

60. Lu, S. Y. & Chipman, R. A. Homogeneous and inhomogeneous Jones matrices. *J. Opt. Soc. Am. A* **11**, 766–773 (1994).
61. Ren, M. X. et al. Reconfigurable metasurfaces that enable light polarization control by light. *Light Sci. Appl.* **6**, e16254 (2017).
62. Genevet, P. et al. Recent advances in planar optics: from plasmonic to dielectric metasurfaces. *Optica* **4**, 139–152 (2017).
63. Balthasar Mueller, J. P. et al. Metasurface polarization optics: independent phase control of arbitrary orthogonal states of polarization. *Phys. Rev. Lett.* **118**, 113901 (2017).
64. He, C. et al. Complex vectorial optics through gradient index lens cascades. *Nat. Commun.* **10**, 4264 (2019).
65. Shen, Y. J. et al. Topologically controlled multiskyrmions in photonic gradient-index lenses. *Phys. Rev. Appl.* **21**, 024025 (2024).
66. Hakobyan, V. & Brasselet, E. Q-plates: from optical vortices to optical skyrmions. *Phys. Rev. Lett.* **134**, 083802 (2025).

Acknowledgements

We would like to acknowledge support from the Department of Engineering Science, University of Oxford and the Royal Society University Research Fellowship (URF\R1\241734) (C.H.).

Author contributions

A.A.W. and C.H. conceived the main ideas. A.A.W., Y.M., Y.Z. and Z.Z. performed the experiments. A.A.W. and C.H. analysed the experimental results and prepared the figures. A.A.W., C.H. and B.D. wrote the paper. A.A.W., Y.M., Y.Z., Z.Z., Y.C., X.Q., B.D. and C.H.

reviewed the results and approved the final version of the manuscript. C.H. supervised the project.

Competing interests
The authors declare no competing interests.

Additional information
Supplementary information The online version contains supplementary material available at https://doi.org/10.1038/s41566-025-01779-x.

Correspondence and requests for materials should be addressed to An Aloysius Wang or Chao He.

Peer review information *Nature Photonics* thanks the anonymous reviewers for their contribution to the peer review of this work.